Published online 15 December 2016

Nucleic Acids Research, 2017, Vol. 45, No. 7 ***e50***
doi: 10.1093/nar/gkw1252

Efficient size-independent chromosome delivery from yeast to cultured cell lines

David M. Brown[1,2], Yujia A. Chan[3,4], Prashant J. Desai[5], Peter Grzesik[5], Lauren M. Oldfield[1], Sanjay Vashee[1], Jeffrey C. Way[4], Pamela A. Silver[3,4] and John I. Glass[1,*]

[1]Synthetic Biology and Bioenergy, J. Craig Venter Institute, Rockville, MD, 20850, USA, [2]Department of Cell Biology and Molecular Genetics, University of Maryland, College Park, MD 20742, USA, [3]Department of Systems Biology, Harvard Medical School, Boston, MA 02115, USA, [4]Wyss Institute for Biologically Inspired Engineering, Boston, MA 02115, USA and [5]Johns Hopkins University, Sidney Kimmel Comprehensive Cancer Center Johns Hopkins, Viral Oncology Program, Baltimore, MD 21231, USA

Received August 17, 2016; Revised October 22, 2016; Editorial Decision November 29, 2016; Accepted December 13, 2016

ABSTRACT

The delivery of large DNA vectors (>100 000 bp) remains a limiting step in the engineering of mammalian cells and the development of human artificial chromosomes (HACs). Yeast is commonly used to assemble genetic constructs in the megabase size range, and has previously been used to transfer constructs directly into cultured cells. We improved this method to efficiently deliver large (1.1 Mb) synthetic yeast centromeric plasmids (YCps) to cultured cell lines at rates similar to that of 12 kb YCps. Synchronizing cells in mitosis improved the delivery efficiency by 10-fold and a statistical design of experiments approach was employed to boost the vector delivery rate by nearly 300-fold from 1/250 000 to 1/840 cells, and subsequently optimize the delivery process for multiple mammalian, avian, and insect cell lines. We adapted this method to rapidly deliver a 152 kb herpes simplex virus 1 genome cloned in yeast into mammalian cells to produce infectious virus.

INTRODUCTION

The delivery of large segments of DNA to the mammalian nucleus remains a significant challenge for gene therapy, large DNA virus reverse genetics, and Human Artificial Chromosome (HAC) development. HACs have been in development since the 1990s to address the limitations of viral-based mammalian vectors (1) and allow megabase-scale cloning capacities, copy number control, and long-term gene expression. The current method for transferring large DNA vectors between cells is microcell-mediated chromosome transfer (MMCT), which is a time-consuming, low efficiency and difficult technique performed by few labs. MMCT works only for select donor rodent cell lines and a limited range of recipient cell lines (2,3). One alternative, polyethylene glycol (PEG)-mediated cell fusion is used to transfer yeast centromeric plasmids (YCps) (4) into cultured mammalian cells, where encoded genes are then expressed (5,6). However, this is conventionally a low efficiency delivery technique (7–10). Other delivery methods such as lipofection (11) and microinjection expose large DNA molecules to shear forces and breakage, decreasing delivery efficiency as the DNA molecule becomes larger requiring the use of agarose plugs to avoid DNA damage due to shear (12–14). In contrast, PEG-mediated fusion does not require isolation and exposure of the YCp to shear damage.

In this report, we sought to enhance the YCp delivery rate for large DNA constructs. There are numerous cellular barriers that prevent the successful delivery of a DNA construct to a mammalian nucleus. We hypothesized that synchronizing cells in M-phase, when the nuclear membrane and cytoskeleton is remodeled, could eliminate a rate-limiting step to achieving successful delivery. Targeting of the nuclear membrane as a barrier for effective DNA delivery has been reported previously through the use of nuclear localization signals (15) and fusogenic proteins (16). In addition, we employed a design of experiments (DoE) methodology to systematically screen and evaluate numerous factors thought to play a role in YCp delivery. Here we describe an improved YCp delivery protocol using PEG-mediated fusion of donor yeast cells with recipient mammalian cells. Our technique increased conventional delivery rates by ∼300-fold for HEK293 cells.

Another necessary step for cell line engineering and HAC development is the synthesis and cloning of large DNA molecules. Efficient genetic tools such as yeast recombination-based assembly methods and capacity of yeast to replicate YCps over 1 Mb (17,18) make *Saccharomyces cerevisiae* a good choice for manipulating large

*To whom correspondence should be addressed. Tel: +1 858 200 1856; Fax: +1 858 200 1880; Email: jglass@jcvi.org

DNA vectors. YCps have diverse utility and have been used to study human genetic elements in transgenic mice (19), assemble exogenous biosynthetic clusters to produce various compounds in yeast (20), and construct entire bacterial genomes, including the 1.1 Mb *Mycoplasma mycoides* bacterial genome (21). In addition, large circular DNA molecules can be assembled from >20 DNA fragments in a single transformation step in yeast (22). Transformation-associated recombination (TAR)-cloning based technology (23–25) was used to assemble the YCps in this study. Using the same organism to both construct and deliver DNA speed up the process and reduces costs.

We further demonstrated the benefits of our improved delivery technique in the field of reverse virus genetics. Generating virus from an engineered viral genome is essential for the study of viral genes, vaccine development, and clinical trials. Viruses with small genomes can readily be obtained by reverse genetics protocols: transfecting cloned viral genes or genomes as plasmids into a susceptible cell culture (26,27). However, larger viruses can be problematic to clone in *Escherichia coli.* Herpes simplex virus type 1 (HSV-1) is a 152 kb double-stranded DNA virus. Using a HSV-1 genome cloned as a YCp, we validated YCp delivery and expression using our improved technique. The infectious HSV-1 genome resulted in generation of infectious virus. We also demonstrated that functional proteins such as the anti-STING VP35 protein (28,29) could be expressed in yeast and delivered simultaneously to mammalian cells alongside the HSV-1 genome to enable infectious virus production in Vero and HeLa cells, which normally do not support HSV-1 replication.

MATERIALS AND METHODS

Yeast strains, cell culture, and materials

The *S. cerevisiae* strain VL6-48 (ATCC MYA-3666: *MATα his3-Δ200 trp1-Δ1 ura3-52 lys2 ade2-1 met14 cir0*) (30) was used for fusions. HEK293 (ATCC CRL-3216) Vero (ATCC CRL-1586), HeLa (ATCC CCL-2), CHO (ATCC CCL-61), A549 (ATCC CCL-185), DF-1 (ATCC CRL-12203) and C6/36 cells (ATCC CRL-1660) were cultured according to manufacturer's instructions supplemented with, 100 units/ml of penicillin, 100 μg/ml of streptomycin, and 0.25 μg/ml Amphotericin B at 37°C and 5% CO_2.

The codon optimized for yeast Ebola-derived VP35 expression vector was synthesized by GenScript (USA) and cloned into pAG413-GPD in yeast (YYC001). Constitutive VP35 expression was confirmed by western blot (data not shown). The test strain (YDB012) was constructed via TAR cloning using pRS313. Test strain YDB123 and YDB1100 were made by inserting approximately 100 kb and 1.1 Mb, respectively of DNA from *Mycoplasma mycoides* (31) via TAR cloning (23–25). A list of plasmids, YCps, and yeast strains can be found in supplementary information (Supplementary Tables S1 and S2).

PEG MW 2000 solution was prepared by adding 12.5 g of PEG 2000 and up to 25 ml of selected HEPES buffer in a 50 ml tube. This was gently shaken until dissolved. PEG solution was kept at room temperature for up to 1 week.

Construction of reporter YCp

We constructed reporter YCps and yeast strains (YDB012, YDB123, YDB1100) that monitor movement of cytoplasmic elements from yeast into mammalian cells. These were circular YCps carrying an mCherry fluorescent protein-encoding gene that is only expressed in yeast using the constitutive GPD (TDH3) promoter, a green fluorescent protein (GFP)-encoding gene under the control of a cytomegalovirus (CMV) promoter only expressed in mammalian cells, and/or stuffer DNA to modulate the vector size. The fluorescent markers were used to quantify the two steps of the delivery process: the fusion rate of yeast spheroplasts and mammalian cells was measured by the post-fusion presence of mCherry in mammalian cells as the yeast cell contents are delivered into the mammalian cytoplasm (Figure 1); the vector delivery rate, which is the rate at which the YCp is delivered to the mammalian nucleus and expressed, was measured by GFP expression in mammalian cells (Figure 1).

Preparation of yeast spheroplasts

Yeast synthetic complete medium lacking histidine, tryptophan and/or uracil, supplemented with adenine (120 mg/l) (Teknova, Inc.) was inoculated with VL6-48 and incubated overnight at 30°C with 200 revolutions per minute (rpm) agitation. The culture was diluted 10-fold with YPD medium (25) and grown to an OD_{600} of 2.0–3.0. Cells were centrifuged at 2500 relative centrifugal force (RCF) for 5 min at 10°C, and the supernatant was decanted. The pellet was resuspended in 20 ml of filter-sterilized 1 M sorbitol and kept at 4°C for 2 h. If needed, cells can be kept at 4°C for up to 24 h with no effect on vector delivery rate. This was pelleted as before and resuspended in 20 ml of SPEM solution (1 M sorbitol, 10 mM EDTA, pH 8.0, 2.08 g/l $Na_2HPO_4{\cdot}7H_2O$ and 0.32 g/l $NaH_2PO_4{\cdot}1H_2O$) with 30 μl of β-mercaptoethanol and 40 μl of Zymolyase-20T solution (200 mg Zymolyase (USB), 9 ml of dH_2O, 1 ml of 1 M Tris–HCl pH 7.5, and 10 ml of 50% glycerol, stored at −20°C). After digestion for 20 min at 30°C with 75 rpm agitation, the OD_{600} was determined for 0.2 ml of SPEM solution containing the yeast cells combined with 0.8 ml of (i) 1 M sorbitol or (ii) 2% SDS solution. The digest continued until the ratio (i/ii) was ∼3–4. 30 ml of 1 M sorbitol was added to the remaining SPEM solution containing the yeast cells and mixed by inversion. Spheroplasts were collected by centrifugation at 1000 RCF for 5 min at 10°C. The pellet was gently resuspended in 50 ml of 1 M sorbitol using a 10-ml pipette and centrifuged as before. Finally, the pellet was resuspended in 2 ml of STC solution (1 M sorbitol, 10 mM Tris–HCl, pH 7.5, 10 mM $CaCl_2$ and 2.5 mM $MgCl_2$) and kept at room temperature for 10–60 min.

YCp delivery protocol for HEK293 cells

Preparation of yeast spheroplasts was completed on the same day as the yeast-HEK293 cell fusion reaction. HEK293 cells were grown in a 75 ml culture flask to 70–80% confluence. Two hours prior to performing the fusion reaction, 6 μL/ml of KaryoMAX® Colcemid™ Solution in

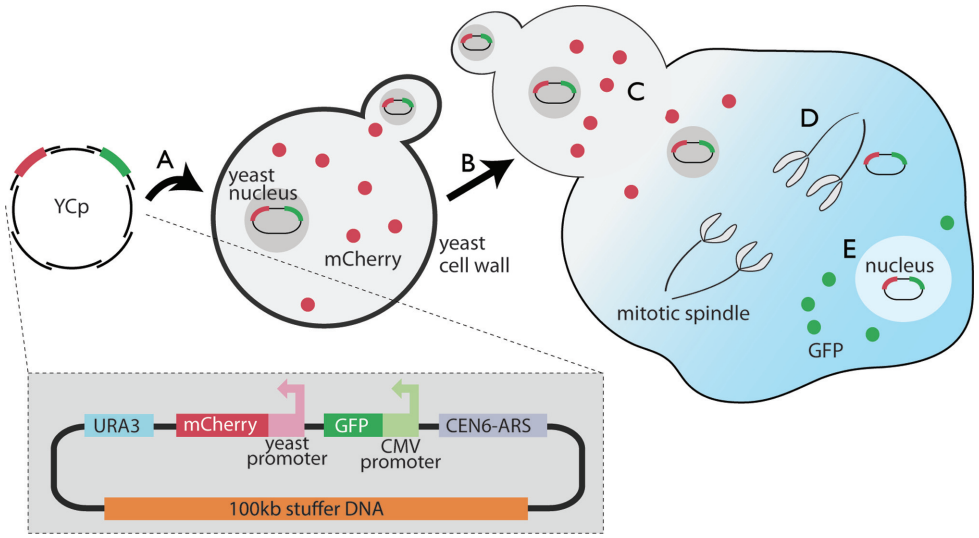

Figure 1. Genetic construct delivery via yeast to mammalian cells. YCp construction and delivery: (**A**) Overlapping genetic constructs are assembled by transformation-associated recombination (TAR) cloning in yeast. (**B**) The yeast spheroplasts are fused to mammalian cells with PEG. (**C**) Delivery of mCherry expressed in yeast to mammalian cells measures the fusion efficiency. (**D**) The construct escapes from the yeast nucleus into the mammalian nucleus. (**E**) GFP expression from the construct indicates vector delivery efficiency.

HBSS (Thermo Scientific) was added to the HEK293 culture. For the fusion reaction, HEK293 cells were trypsinized using 0.25% Trypsin–EDTA (Thermo Fisher). HEK293 cells and yeast spheroplasts were counted on a hemocytometer. One million HEK293 cells were centrifuged in a 1.5 ml tube at 1957 RCF for 1 min and washed with phosphate buffered saline pH 7.4 (PBS) (Gibco). Yeast spheroplasts were added to PBS and mixed with the HEK293 cells so that the ratio of yeast to HEK293 cells was 100:1. The number of yeast spheroplasts was determined using a spectrophotometer at OD_{600} after normalizing by counting spheroplasts on a hemocytometer. Typically, this involved using 50–200 ul of prepared spheroplasts in STC. This was centrifuged as before and the supernatant was decanted. 50 μl of DMSO (Sigma) and 450 μl of PEG MW 2000 solution (12.5 g of PEG 2000 (Aldrich) in 25 ml of HEPES buffer kept at room temperature up to 1 week) was added to the cell mixture and mixed by pipetting. No >1 min was allowed to pass before adding 1 ml of serum free HEK293 media. This was centrifuged as before, the supernatant was decanted, and the cell pellet was resuspended in 1 ml of HEK293 media for plating into a 6-well tissue culture plate. The media was replaced after 12 h. Evidence of YCp delivery can be seen 48 h post-fusion. The vector delivery rate was determined by counting the number of GFP fluorescent cells and comparing that number to the number of recipient cells used in the fusion.

Optimized YCp delivery protocol for Vero cells

The protocol for Vero cells was modified from the HEK293 protocol as follows: 24 h prior to fusion, 50 μl of KaryoMAX® Colcemid™ Solution was added to the Vero cell culture. Then, Vero media was removed and reserved in a 50 ml tube. Vero cells were trypsinized according to the manufacturer's instructions using Trypsin–EDTA (0.25%) and phenol red (Thermo Fisher), and resuspended in the reserved media. After the step where yeast was added, 5 minutes were allowed to pass before centrifugation. PEG-cell mixture was placed at 30°C for 5.5 min before adding 1 ml of serum-free Vero media.

Optimized YAC delivery protocol for C6/36 cells

The protocol for C6/36 cells was modified from the Vero protocol as follows: The ratio of yeast cells to C6/36 cells was 50:1. After the step where yeast was added, 5 min were allowed to pass before centrifugation. After the step where PEG solution was added, 5 min were allowed to pass before adding 1 ml serum free C6/36 media.

Fractional factorial design

Fractional factorial designs or more specifically Plackett–Burman designs of resolution III were used for screening studies these are powerful design of experiment (DOE) tools to estimate the effects of several factors. Resolution III designs do not confound with main effects however there may be confounding with two-factor interactions (32,33). Resolution III was used due to the large number of factors being tested. Designs were created in JMP 10.0 (SAS institute Inc., Cary, NC, USA) and used to screen for important factors prior to optimization and OFAT analysis. The independent variables were studied at two or three different levels; low (−1), medium (0), and high (+1). The designs can be seen for HEK-293 cells (Supplementary Table S3) Vero cells (Supplementary Table S4) and C6/36 cells (Supplementary Table S5).

Response surface methodology (RSM)

RSM based on a custom central composite design with six coded levels was employed to determine the optimal conditions of the screened factors in the Plackett–Burman

and/or fractional factorial designs. All models and analysis were performed with JMP statistical software version 10.0.0 (SAS Institute Inc., Cary, NC, USA). The final experimental design consisted of 23 runs varying two of the most significant factors identified (Supplementary Table S6). Statistical significance was checked by *F*-test, ANOVA, and goodness of fit.

Detection of HSV-1 virus replication

The HSV-1 genome was constructed in yeast as a YCp and delivered to recipient cells. The recipient cells were harvested after 4 days: freeze-thawed once and sonicated in a cup horn sonicator. Virus in the lysate were enumerated using serial dilutions in PBS that were plated on Vero cell monolayers in tissue culture trays. Following absorption, the culture was overlayed with carboxymethylcellulose in growth medium and incubated for 4 days. Plaques were visualized by crystal violet stain. Viral titers were determined by $TCID_{50}$ assay using Vero cells.

Determining fusion rate of HEK293 using flow cytometry or fluorescence microscopy

Upon fusing HEK293 cells with the optimized YCp delivery protocol, samples were plated into a six-well tissue culture plate. After HEK293 cells adhered to the plate (3–4 h post-fusion), excess yeast was removed by washing HEK293 cells with medium, and then adding fresh medium. Plates were observed on a Nikon eclipse Ti fluorescence microscope. To prepare samples for flow cytometry fused HEK293 cells were trypsinized, filtered using a 70 μm filter (Corning), washed, and resuspended in PBS. Using an Accuri C6 flow cytometer (BD Bio-sciences), we analyzed post-fusion cell cultures. Analysis was based on light-scatter and fluorescence signals produced from 20 mW laser illumination at 488 nm. A 670 nm long-pass filter was used to detect mCherry. Threshold levels were empirically set to eliminate detection of yeast cells and debris. The flow cytometer was routinely operated at the slow flow rate setting (14 l sample/minute). Data acquisition for a single sample took 3–5 min.

Mitotic index experiments

Several concentrations of colcemid, nocodazole, STLC, or okadaic acid were added directly to the media of a HEK293 cells growing in a 96-well plate. Two hours after treatment with the drug, cells were fixed in 4% (w/v) PFA (paraformaldehyde, Merck) solution followed by a second fixation with ice cold methanol-acetone 1:1 mix for 5 min at −20°C. After PBS washing, cells permeabilized with PBS–0.1% (v/v) Triton X 100 for 5 min, and were blocked with PBS-3% (w/v) BSA for 30 min at room temperature. After PBS washing, cells were stained with DAPI (4′, 6-diamino-2-phenylindole dihydrochloride; 100 ng/ml; Sigma) for 5 min at room temperature protected from light. The mitotic index was measured by counting the number of cells with condensed chromosomes, and percentages calculated. At least four fields comprising a total of >100 cells were analyzed for each measurement. Plates were observed on a Nikon eclipse Ti fluorescence microscope.

RESULTS

Synchronizing mammalian cells in mitosis improves vector delivery

Using drugs to synchronize mammalian cells in mitosis prior to fusion with yeast spheroplasts resulted in a 10–25-fold increase in vector delivery rates (Figure 2); Colcemid (Gibco), which inhibits microtubule polymerization (34), *S*-trityl-L-cysteine (STLC) (Sigma), a kinesin 5 inhibitor (35) and nocodazole (Sigma), another microtubule polymerization inhibitor (36) all improved vector delivery rates at different optimum concentrations. Okadaic acid (Sigma), which inhibits serine/threonine phosphatases and synchronizes cells in G1/S-phase at high concentrations (37,38), did not improve vector delivery at low concentrations and eliminated vector delivery at high concentrations, indicating that mitotic arrest and nuclear envelope breakdown are required for efficient vector delivery. Calculation of the mitotic index for each mitotic drug by analysis of condensed chromosomes (Supplementary Figure S3) showed that 2 h of treatment with nocodazole, STLC or colcemid presented an index of ∼20% at different minimum concentrations. As the concentration of each drug increased the mitotic index increased until leveling off for each drug at ∼20%, untreated cells presented an index of 5%. The optimum concentration for each drug for YCp delivery was approximately the lowest concentration necessary to enhance the mitotic index to 20%. Subsequent experiments were carried out with Colcemid as it was observed to produce consistently higher rates of delivery.

Design of experiments optimizing delivery in multiple cell lines

The conventional 'one-factor-at-a-time' (OFAT) approach, in which one independent variable is studied while maintaining all the other factors at a constant level, is frequently used in biotechnology to obtain higher product yields or to optimize a process. However, OFAT is time consuming, and disregards potential complex interactions among factors. Design of experiments (DoE) is a collection of statistical techniques and methods that can be used to overcome these problems reducing time and cost in process optimization (32,33,39). DoE is performed in two main stages. First, a fractional factorial design is used to screen for the main effects and to eliminate factors that have no or little effect on the process. Second, a higher resolution experiment using response surface methodology (RSM) is performed with fewer factors to obtain an optimized protocol. Using this methodology, fewer experimental trials are needed compared with OFAT and potential interactions among factors can be identified. Factors tested were primarily selected from differences reported from various protocols of YCp or YAC delivery (7–10,40–44).

HEK293 cells were the first cell line optimized for vector delivery. Factors were first screened using a fractional factorial design (Supplementary Table S3) and the regression results (Supplementary Table S7) predicted the major effects on vector delivery. Using either an OFAT approach or a fractional factorial design eighteen factors were systematically tested for their effect on the post-fusion fraction

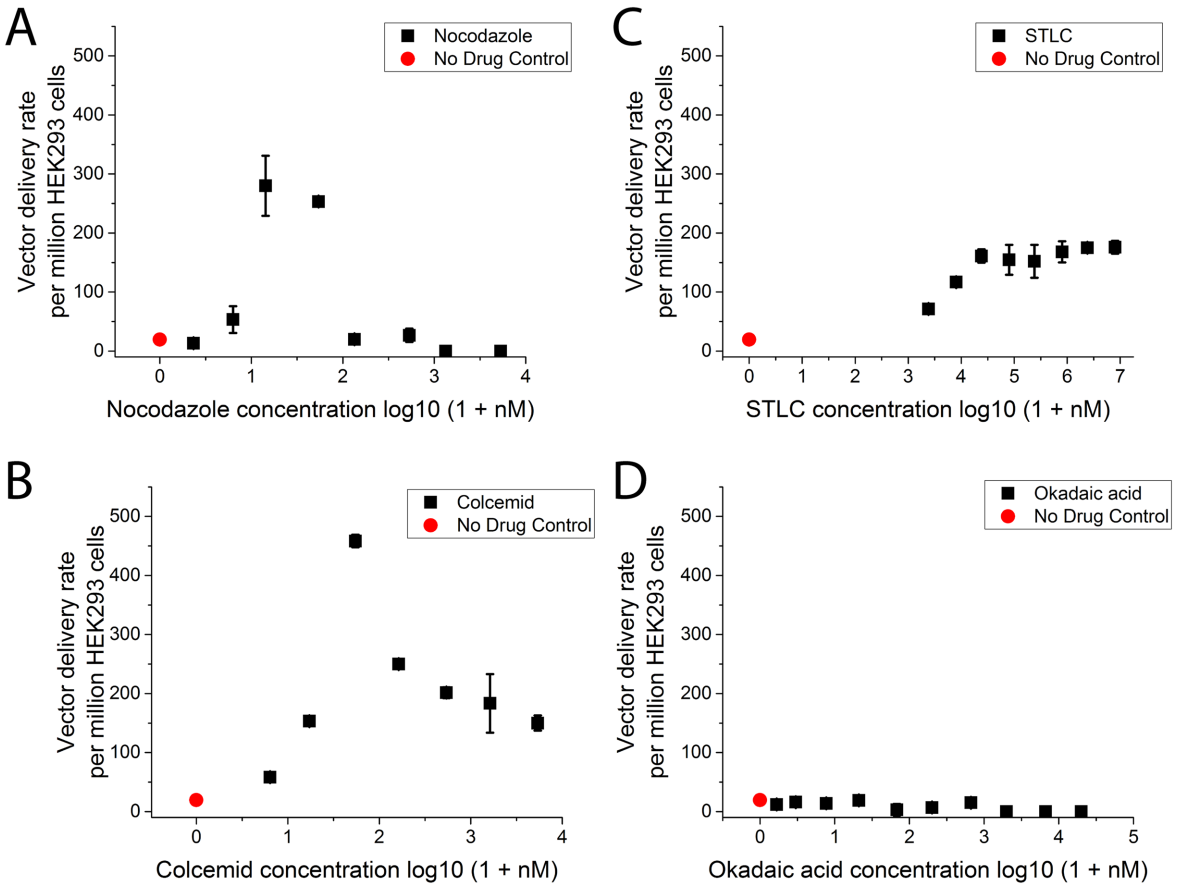

Figure 2. Mitotic arrest of mammalian cells significantly increases the vector delivery rate. Vector delivery rate was determined by counting the number of recipient cells expressing the delivered fluorescent reporter. Colcemid (**A**), STLC (**B**) and nocodazole (**C**) arrest cells in mitosis. Okadaic acid (**D**) arrests cells in S-phase. Colcemid at 54 nM most strongly enhanced vector delivery efficiency. Error bars represent the standard deviation of four replicates.

of mammalian cells expressing GFP (Table 1). The most critical continuous factor identified was the ratio of yeast spheroplasts to recipient cells. Using an OFAT experiment, the vector delivery rate peaked when the yeast to mammalian cell ratio was 100:1 (Figure 3). A higher cell ratio adversely affects vector delivery and post-fusion cell viability likely due to nutrient competition from the excess yeast. We observed the same result when measuring fusion efficiency, which we define as the fraction of mCherry-positive HEK293 cells in the total population. Increasing the ratio of yeast to recipient cells 3-fold decreased the fusion efficiency from 20% to 2% (Figure 4, Supplementary Figure S1). When observing GFP expression as a measure of vector delivery rate, mCherry can still be observed dimly in cells 48 h post fusion; however, the magnitude of fluorescence is significantly reduced from 24 h post fusion.

Fusion time was also identified as a highly significant factor (P-value = 0.0039). Several categorical factors were also identified as highly significant; diluting the media after adding PEG, osmotically stabilizing the yeast cells in sorbitol and the use of the fungicide Amphotericin B in media. Major factors were optimized by OFAT or RSM (data not shown), which predicted the optimal yeast to mammalian cell ratio, PEG incubation time, and cell line-specific conditions (Table 1). The vector was delivered and expressed in

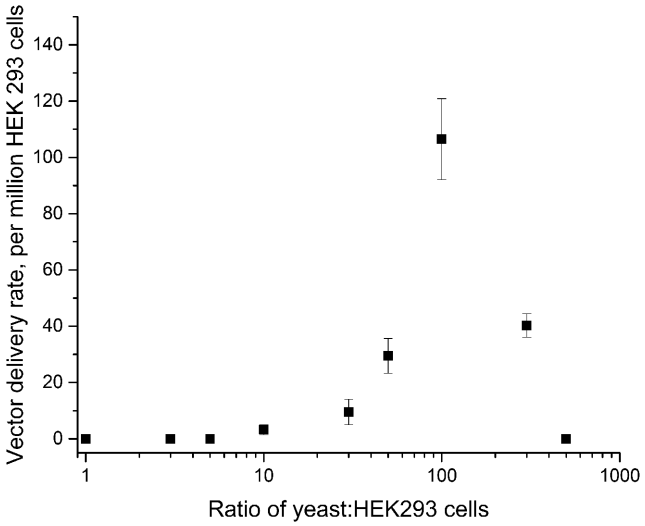

Figure 3. The vector delivery rate is significantly affected by the ratio of yeast to recipient cells. The optimal ratio of yeast to HEK293 cells was 100:1. Error bars represent the standard deviation of four replicates.

1210 ± 60 yeast cells per million HEK293 cells using the optimized protocol.

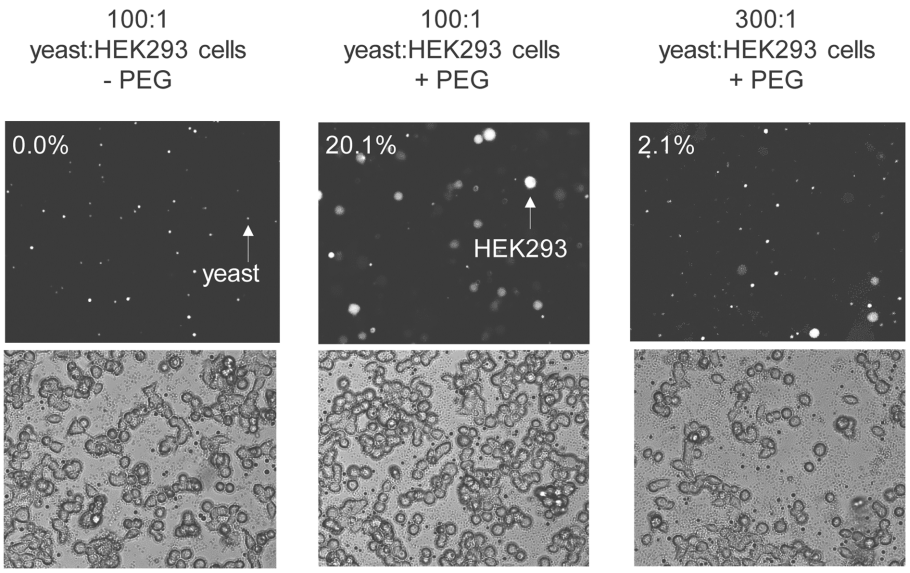

Figure 4. Fusion efficiency is significantly affected by the ratio of yeast to recipient cells. The fusion efficiency was determined by the percentage of mCherry-positive HEK293 cells post-fusion. Microscopy images at 200× magnification show mCherry fluorescence (top panels) and differential interference contrast (DIC; bottom panels). The percentage of HEK293 cells that were mCherry-positive post-fusion is stated on the top left corner and was determined by counting mCherry-positive and negative cells on a hemocytometer. The PEG incubation time, HEK293 cell number and yeast to HEK293 cell ratio were 1 min, 1×10^5 cells and 100:1, respectively.

Table 1. Significance of factors impacting vector delivery and recipient cell viability for HEK293 cells

Factor	*P*-value	*P*-value source	Optimized condition for HEK293 cells	Range of conditions tested
Concentration of drug	<0.001*	OFAT	(Figure 2)	(Figure 2)
Ratio of yeast to recipient cells	<0.001*	OFAT	100:1	1:1000–1:1
Fusion time	<0.001*	Fractional factorial	1 min	1–20 min
PEG concentration	<0.001*	OFAT	50%	20–50%
PEG molecular weight	<0.001*	OFAT	2000 g/mol	1000–8000 g/mol
PEG buffer	<0.001*	OFAT	25 mM HEPES	10–100 mM HEPES and Tris
Use of Amphotericin B in media	<0.001*	OFAT	2.5 μg/ml	0-2.5 μg/ml
Dilute media after adding PEG	0.0469*	Fractional factorial	Dilute with 1 ml	Dilution versus no dilution
Osmotically stabilize in sorbitol	0.0808	Fractional factorial	Stabilize at 4°C for 16 h	Stabilize at 4°C for 0–24 h
Pre-fusion incubation time	0.2789	Fractional factorial	1 min	1–20 min
Calcium concentration	0.3643	Fractional factorial	0 M	0–0.1 M
DMSO amount	0.4032	Fractional factorial	10%	0–10%
Replace media after 12 h	0.4051	Fractional factorial	Replace with DMEM + 10% FBS	Replacement versus no replacement
Stirring during PEG incubation	0.4431	Fractional factorial	Stirring not necessary	Stirring versus no stirring
Recovery time	0.4892	Fractional factorial	All conditions tested	0–5 min
FBS amount	0.6071	OFAT	All conditions tested	5–10%
Recovery temperature	0.837	Fractional factorial	25°C	4–42°C
PEG incubation temperature	0.8798	Fractional factorial	25°C	25–42°C
Yeast growth phase	0.928	Fractional factorial	All conditions tested	Log to stationary phase

(OFAT – One Factor At a Time).

Vero cells were optimized following a similar methodology. The initial vector delivery rate (2.0 ± 0.7 per 300 000 cells) using the HEK293 optimized protocol was too low to muster sufficient statistical power in the fractional factorial design to identify major factors. Therefore, initially we optimized the treatment with mitotic arrest drugs and the ratio of yeast to Vero cells by OFAT (data not shown). Following initial optimization via OFAT, eight factors were evaluated by a Plackett–Burman fractional factorial resolution III design (Supplementary Table S4). Significant categorical factors that were identified when optimizing HEK293 cells were not optimized for Vero cells since it was highly unlikely the condition that resulted in no YCp delivery would be advantageous in delivering YCps to Vero cells. Regres-

sion results from the Plackett-Burman design identified and eliminated non-major factors (Supplementary Table S8). A resolution V RSM design (Supplementary Table S6) was used with the major factors identified optimized the protocol (Supplementary Figure S2). The model obtained had a very low *P*-value (<0.001) and the lack of fit *P*-value of 0.063 implied that the lack of fit was not significant relative to the pure error (Supplementary Table S9). A ∼100× improvement of the vector delivery rate for Vero cells was obtained when using the Vero-specific protocol compared to the HEK293-specific protocol (Table 2).

Optimizing Vero cells created a pipeline for the optimization of new cell lines. The insect cell line C6/36 followed this pipeline to create an optimized protocol. The initial vector delivery rate was 1.5 ± 1.0 per 300,000 cells using the HEK293 protocol. First, OFAT optimize the treatment with mitotic arrest drugs. The differences in the efficiency of synchronizing cells in mitosis could explain differences in YCp delivery rates between different cell lines (45). Second, evaluate major factors (Supplementary Table S10) by a Plackett-Burman fractional factorial design (Supplementary Table S5). Third, use the central composite RSM design (Supplementary Table S6) to optimize PEG incubation time and cell ratio. ANOVA results (*P*-value = 0.0021) for C6/36 are given in (Supplementary Table S11). The optimized C6/36 protocol improved the vector delivery rate to 112 ± 14 per 300 000 cells. The central composite RSM design was also evaluated using HEK293 cells (Supplementary Table S12) and gave a *P*-value = 0.0021.

Vector delivery rate was independent of vector size

We found that the vector delivery rate was independent of vector size. *M. mycoides* genomic DNA was used to modulate the size of the YCp between 0.1–1.1 Mb. *Mycoplasma* DNA should be transcriptionally and translationally inert in eukaryotic cells due to its bacterial origin and non-standard genetic code (46). The vector delivery rate in HEK293 cells remained constant at all tested YCp sizes (12 kb; YDB012, 100 kb; YDB123, or 1.1 Mb; YDB1100) (Table 2). The YCp was confirmed to be delivered intact using multiplex PCR amplification on eight sites distributed along the 1.1 Mb YCp (47). Seventy-two hours post fusion, lysed HEK293 cells were used as a template. Each primer set (Supplementary Table S13) amplifies a segment at least 100 kb from any other set, spanning the entire 1.1 Mb YCp (Supplementary Figure S4).

Delivery of the HSV-1 genome via fusion produced infectious virus

GFP synthesis from the delivered YCps demonstrates that mammalian polymerases can transcribe the YCp delivered to the mammalian cells as yeast chromatin. This indicates that transit and packaging in yeast does not interfere with mammalian expression as has been previously suggested (5,6). As a next step, we tested whether YCps delivered to mammalian cells as yeast chromatin could be replicated in the mammalian cell. Naked herpes virus DNA is infectious when transfected into mammalian cells (48–50). We delivered a HSV-1 genome assembled as a YCp from yeast

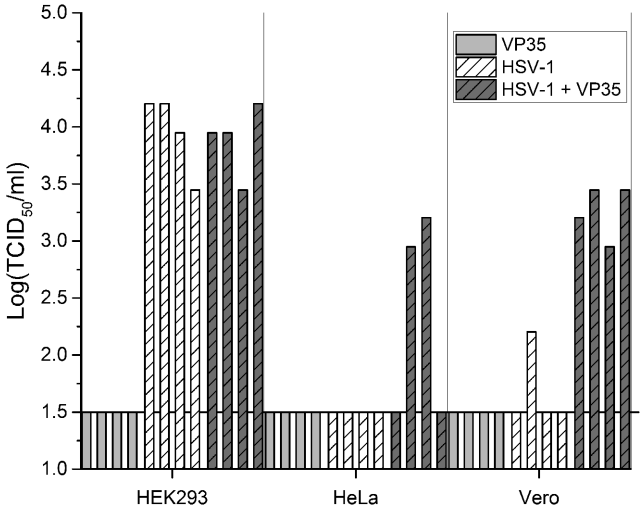

Figure 5. VP35 enhances HSV-1 generation from a viral genome cloned in and delivered by yeast. HEK293, HeLa, or Vero cells were fused with a yeast strain containing the HSV-1 genome and/or a VP35 expression plasmid. Supernatants were collected 72 h post-fusion and viral titer was determined. The limit of detection is indicated by the solid horizontal line. Samples that produced no virus are indicated at the limit of detection. Each condition had four replicates.

to mammalian cells. HSV-1 plaques appeared 4 days post-passage as indicative of infectious virus production (Supplementary Figure S5A). This demonstrated that the delivered YCps could be recognized and replicated by viral DNA polymerases and used to generate virus from cloned large viral genomes.

Exogenous DNA that enters mammalian cells is commonly silenced via the STING (Stimulator of Interferon Genes) pathway (51,52), which facilitates interferon production in response to cytosolic naked DNA or RNA from viruses. Supplying DNA as yeast chromatin may avoid gene silencing to a certain extent. In HEK293 cells, we were able to produce HSV-1 via fusion with yeast carrying the HSV-1 YCp. However, HeLa cells did not produce virus after fusion. This is likely because the STING pathway is not highly activated in HEK-293 cells (53).

To counter STING-mediated silencing, fusion experiments were performed with yeast expressing the Ebola-derived VP35 protein, which inhibits the activation of IRF-3 kinases and the IFN-beta promoter downstream of STING (28,29). Fusion using a yeast strain that expressed VP35 protein and harbored the HSV-1 genome enabled HSV-1 production in HeLa cells and enhanced the frequency of virus generation in Vero cells. In Vero cells, virus was observed in only one of four trials without VP35, versus in all 4 trials with VP35; viral titers were also higher (Figure 5). We demonstrated that the delivery of proteins and genomes could be modularized: the VP35 could be expressed in yeast separate from the yeast harboring the HSV-1 genome. Fusion experiments using both strains of yeast resulted in similar HSV-1 genome expression compared to fusion using a strain of yeast that expressed VP35 and carried the HSV-1 genome (Supplementary Figure S5B).

Table 2. Vector delivery efficiency according to cell line and vector size

Cell line	Fusion protocol optimized for	Number of reporter expressing cells observed (per 300,000)	Vector size
HEK293	HEK293	326 ± 26*	1.1 Mb
HEK293	HEK293	364 ± 19*	100 kb
HEK293	HEK293	341 ± 21*	12 kb
HEK293	HEK293	0	No vector
HEK293	Vero	23 ± 6	100 kb
HEK293	C6/36	32 ± 8	100 kb
HeLa	HEK293	3.5 ± 2	100 kb
CHO	HEK293	3.0 ± 0.7	100 kb
A549	HEK293	1.5 ± 0.5	100 kb
Vero	HEK293	2.0 ± 0.7	100 kb
Vero	Vero	102 ± 6	100 kb
C6/36 (insect)	HEK293	1.5 ± 1.0	100 kb
C6/36 (insect)	C6/36	112 ± 14	100 kb
DF-1 (chicken)	C6/36	1.0 ± 0.5	100 kb
DF-1 (chicken)	HEK293	0	100 kb
DF-1 (chicken)	Vero	0	100 kb

*No significant difference (F ratio = 2.15, F *critical* = 5.14, P-value = 0.1975).

DISCUSSION

In this work, we developed an efficient method for transferring large YCps from yeast to different cell lines. PEG-mediated fusion eliminates the need for the vector to cross the cytoplasmic membranes of the donor and recipient cells. It also avoids hydrodynamic shear forces damaging DNA molecules, which could happen when genomic DNA is isolated from cells prior to transfer. We improved vector delivery by arresting the recipient mammalian cell in the M-phase of the cell cycle when the mammalian nuclear envelope is broken down, thus allowing for easier diffusion of the vector to where the mammalian nucleus re-forms. We used three different mitotic arrest drugs: Colcemid and nocodozole both interfere with microtubule polymerization. STLC synchronizes cells by inhibiting kinesin 5. The different drug mechanisms suggest that there is not another confounding variable causing an increase in vector delivery rate. This was confirmed upon analyzing the mitotic index of each drug. Each drug had a different minimum effective concentration, increasing the mitotic index from 5% to 20%. The optimum concentration for each drug for vector delivery correlated to this minimum effective concentration. However, as the concentration of microtubule interfering drugs increased, the mitotic index remained unchanged as the vector delivery rate decreased possibly due to cellular toxicity. The differences in vector delivery rate between each drug could not be completely explained by mitotic index.

Subtle differences in protocol can have a significant effect on vector delivery. We employed DoE along with OFAT to improve fusion efficiencies for three different cell lines. The pipeline and optimization protocol presented here provides a versatile protocol that could be utilized to optimize vector delivery to other cell types. In addition, an insect and avian cell line were also amenable to delivery, suggesting that the protocol may be applicable to other animal phyla.

The ability to deliver functional proteins expressed in yeast alongside genetic constructs assembled in yeast will advance and diversify the tools for gene delivery to mammalian cells. We showed that VP35 protein delivery made HSV-1 genome delivery and expression possible in HeLa cells where it was previously undetectable when the HSV-1 genome was delivered alone. VP35 co-delivery also enhanced HSV-1 production in Vero cells. As expected, delivery rates in HEK293 cells were unimproved by VP35 co-delivery because HEK293 cells have low or undetectable cGAS and STING protein levels (53). We determined that the co-delivery of protein and DNA within the same yeast cell was not required. Because of the high yeast to recipient cell ratio, one yeast strain can deliver the VP35 and the other can deliver the DNA. This is likely due to the high fusion efficiency (20% of recipient cells obtain fluorescent protein in the yeast cytoplasm after fusion) relative to the lower DNA delivery rate. The co-delivery of other proteins that alter cellular processes resulting in protection of exogenous DNA may be equally useful for reverse virus genetics or HACs. There is also the potential to engineer fusion proteins that can bind to the genetic constructs and target their delivery into the mammalian cell nucleus using a nuclear localization sequence. Our method of fusing yeast to recipient cells makes the co-delivery of functional proteins an easy and effective option.

We used the delivery of yeast carrying HSV-1 genomic DNA as a surrogate for a HAC (in development). We showed that yeast chromatin can be replicated by a HSV-1 DNA polymerase that evolved to replicate DNA associated with mammalian histones and other nuclear associated proteins (54). This suggests that HACs delivered into mammalian cells using yeast vectors will similarly be processed by mammalian DNA replication machinery. In addition to answering our questions about the compatibility of yeast chromatin with mammalian DNA polymerases, these experiments also offer new possibilities for doing reverse genetics of viruses with large DNA genomes such as other herpes viruses, pox viruses, and the African Swine Fever Virus.

This improved protocol can be a powerful tool for the delivery of large DNA molecules into mammalian cells. MMCT, the method most commonly used for the delivery of HACs into mammalian cells has a yield frequency of no greater than 1/1 000 000–1/100 000 (16,55) although recent advancements have reported improved delivery efficiencies (56,57). We boosted YCp vector delivery rate to

1/840 for HEK293 cells. Importantly, we are able to consistently obtain efficient YCp delivery and showed that vector sizes up to 1.1 Mb do not impede the YCp delivery rate. The largest reported YCp is 2.3 Mb (5), and is likely not an upper limit or obstacle for our technique. We demonstrated that this protocol could be reliably optimized for different cell lines from higher eukaryotes (Table 2). It is likely that following the described optimization pipeline many more cell lines can be optimized. The YCp delivery method represents an inexpensive and rapid technique that can be replicated in most laboratories without specialized equipment. YCp-based vector delivery will be useful for studies of gene cluster regulation, transgenic animal construction, and *de novo* HAC development. Advances in the synthesis of mammalian chromosomes in yeast cells will be complemented by this approach for chromosome delivery from yeast to animal cells.

SUPPLEMENTARY DATA

Supplementary Data are available at NAR Online.

ACKNOWLEDGEMENTS

We thank Clovis Basier for assistance in illustrating Figure 1. We thank Devin R. Burrill for her insightful comments on the manuscript. We thank Reed S. Shabman for reagents and for providing the C6/36 *Aedes albopictus* cell line.

FUNDING

Defense Advanced Research Projects Agency [W911NF-11-2-0056]; National Institutes of Health [R01GM036373-32, R21AI109418-01]; J. Craig Venter Institute; Human Frontier Science Program Postdoctoral Fellowship [LT000168/2015-L to Y.A.C.]. Funding for open access charge: The J. Craig Venter Institute.
Conflict of interest statement. None declared.

REFERENCES

1. Kouprina,N., Earnshaw,W.C., Masumoto,H. and Larionov,V. (2013) A new generation of human artificial chromosomes for functional genomics and gene therapy. *Cell. Mol. Life Sci.*, **70**, 1135–1148.
2. Meaburn,K.J., Parris,C.N. and Bridger,J.M. (2005) The manipulation of chromosomes by mankind: the uses of microcell-mediated chromosome transfer. *Chromosoma*, **114**, 263–274.
3. Fournier,R.E. and Ruddle,F.H. (1977) Microcell-mediated transfer of murine chromosomes into mouse, Chinese hamster, and human somatic cells. *Proc. Natl. Acad. Sci. U.S.A.*, **74**, 319–323.
4. Christianson,T.W., Sikorski,R.S., Dante,M., Shero,J.H. and Hieter,P. (1992) Multifunctional yeast high-copy-number shuttle vectors. *Gene*, **110**, 119–122.
5. Marschall,P., Malik,N. and Larin,Z. (1999) Transfer of YACs up to 2.3 Mb intact into human cells with polyethylenimine. *Gene Ther.*, **6**, 1634–1637.
6. Kazuki,Y., Hoshiya,H., Takiguchi,M., Abe,S., Iida,Y., Osaki,M., Katoh,M., Hiratsuka,M., Shirayoshi,Y., Hiramatsu,K. *et al.* (2011) Refined human artificial chromosome vectors for gene therapy and animal transgenesis. *Gene Ther.*, **18**, 384–393.
7. Davies,N.P., Rosewell,I.R. and Bruggemann,M. (1992) Targeted alterations in yeast artificial chromosomes for inter-species gene transfer. *Nucleic Acids Res.*, **20**, 2693–2698.
8. Julicher,K., Vieten,L., Brocker,F., Bardenheuer,W., Schutte,J. and Opalka,B. (1997) Yeast artificial chromosome transfer into human renal carcinoma cells by spheroplast fusion. *Genomics*, **43**, 95–98.
9. Huxley,C., Hagino,Y., Schlessinger,D. and Olson,M.V. (1991) The human HPRT gene on a yeast artificial chromosome is functional when transferred to mouse cells by cell fusion. *Genomics*, **9**, 742–750.
10. Auriche,C., Carpani,D., Conese,M., Caci,E., Zegarra-Moran,O., Donini,P. and Ascenzioni,F. (2002) Functional human CFTR produced by a stable minichromosome. *EMBO Rep.*, **3**, 862–868.
11. Zabner,J., Fasbender,A.J., Moninger,T., Poellinger,K.A. and Welsh,M.J. (1995) Cellular and molecular barriers to gene transfer by a cationic lipid. *J. Biol. Chem.*, **270**, 18997–19007.
12. Rocchi,L., Braz,C., Cattani,S., Ramalho,A., Christan,S., Edlinger,M., Ascenzioni,F., Laner,A., Kraner,S., Amaral,M. *et al.* (2010) Escherichia coli-cloned CFTR loci relevant for human artificial chromosome therapy. *Hum. Gene Ther.*, **21**, 1077–1092.
13. Bauchwitz,R. and Costantini,F. (1998) YAC transgenesis: a study of conditions to protect YAC DNA from breakage and a protocol for transfection. *Biochim. Biophys. Acta*, **1401**, 21–37.
14. Karas,B.J., Jablanovic,J., Irvine,E., Sun,L., Ma,L., Weyman,P.D., Gibson,D.G., Glass,J.I., Venter,J.C., Hutchison,C.A. 3rd *et al.* (2014) Transferring whole genomes from bacteria to yeast spheroplasts using entire bacterial cells to reduce DNA shearing. *Nat. Protoc.*, **9**, 743–750.
15. Miller,A.M. and Dean,D.A. (2009) Tissue-specific and transcription factor-mediated nuclear entry of DNA. *Adv. Drug Deliv. Rev.*, **61**, 603–613.
16. Hiratsuka,M., Ueda,K., Uno,N., Uno,K., Fukuhara,S., Kurosaki,H., Takehara,S., Osaki,M., Kazuki,Y., Kurosawa,Y. *et al.* (2015) Retargeting of microcell fusion towards recipient cell-oriented transfer of human artificial chromosome. *BMC Biotechnol.*, **15**, 58.
17. Burke,D.T., Carle,G.F. and Olson,M.V. (1987) Cloning of large segments of exogenous DNA into yeast by means of artificial chromosome vectors. *Science*, **236**, 806–812.
18. Larin,Z., Monaco,A.P. and Lehrach,H. (1991) Yeast artificial chromosome libraries containing large inserts from mouse and human DNA. *Proc. Natl. Acad. Sci. U.S.A.*, **88**, 4123–4127.
19. Li,L. and Blankenstein,T. (2013) Generation of transgenic mice with megabase-sized human yeast artificial chromosomes by yeast spheroplast-embryonic stem cell fusion. *Nat. Protoc.*, **8**, 1567–1582.
20. Goldman,S. (2010) Genetic chemistry: production of non-native compounds in yeast. *Curr. Opin. Chem. Biol.*, **14**, 390–395.
21. Gibson,D.G., Benders,G.A., Andrews-Pfannkoch,C., Denisova,E.A., Baden-Tillson,H., Zaveri,J., Stockwell,T.B., Brownley,A., Thomas,D.W., Algire,M.A. *et al.* (2008) Complete chemical synthesis, assembly, and cloning of a Mycoplasma genitalium genome. *Science*, **319**, 1215–1220.
22. Gibson,D.G., Benders,G.A., Axelrod,K.C., Zaveri,J., Algire,M.A., Moodie,M., Montague,M.G., Venter,J.C., Smith,H.O. and Hutchison,C.A. 3rd (2008) One-step assembly in yeast of 25 overlapping DNA fragments to form a complete synthetic Mycoplasma genitalium genome. *Proc. Natl. Acad. Sci. U.S.A.*, **105**, 20404–20409.
23. Noskov,V.N., Ma,L., Chen,S. and Chuang,R.Y. (2015) Recombinase-mediated cassette exchange (RMCE) system for functional genomics studies in Mycoplasma mycoides. *Biol. Proc. Online*, **17**, 6.
24. Lee,N.C., Larionov,V. and Kouprina,N. (2015) Highly efficient CRISPR/Cas9-mediated TAR cloning of genes and chromosomal loci from complex genomes in yeast. *Nucleic Acids Res.*, **43**, e55.
25. Kouprina,N. and Larionov,V. (2008) Selective isolation of genomic loci from complex genomes by transformation-associated recombination cloning in the yeast Saccharomyces cerevisiae. *Nat. Protoc.*, **3**, 371–377.
26. Neumann,G., Watanabe,T., Ito,H., Watanabe,S., Goto,H., Gao,P., Hughes,M., Perez,D.R., Donis,R., Hoffmann,E. *et al.* (1999) Generation of influenza A viruses entirely from cloned cDNAs. *Proc. Natl. Acad. Sci. U.S.A.*, **96**, 9345–9350.
27. Zhang,X., Kong,W., Ashraf,S. and Curtiss,R. 3rd (2009) A one-plasmid system to generate influenza virus in cultured chicken cells for potential use in influenza vaccine. *J. Virol.*, **83**, 9296–9303.
28. Cardenas,W.B., Loo,Y.M., Gale,M. Jr, Hartman,A.L., Kimberlin,C.R., Martinez-Sobrido,L., Saphire,E.O. and Basler,C.F. (2006) Ebola virus VP35 protein binds double-stranded RNA and inhibits alpha/beta interferon production induced by RIG-I signaling. *J. Virol.*, **80**, 5168–5178.

29. Basler,C.F., Mikulasova,A., Martinez-Sobrido,L., Paragas,J., Muhlberger,E., Bray,M., Klenk,H.D., Palese,P. and Garcia-Sastre,A. (2003) The Ebola virus VP35 protein inhibits activation of interferon regulatory factor 3. *J. Virol.*, **77**, 7945–7956.
30. Larionov,V., Kouprina,N., Solomon,G., Barrett,J.C. and Resnick,M.A. (1997) Direct isolation of human BRCA2 gene by transformation-associated recombination in yeast. *Proc. Natl. Acad. Sci. U.S.A.*, **94**, 7384–7387.
31. Gibson,D.G., Glass,J.I., Lartigue,C., Noskov,V.N., Chuang,R.Y., Algire,M.A., Benders,G.A., Montague,M.G., Ma,L., Moodie,M.M. *et al.* (2010) Creation of a bacterial cell controlled by a chemically synthesized genome. *Science*, **329**, 52–56.
32. Plackett,R.L. and Burman,J.P. (1946) The design of optimum multifactorial experiments. *Biometrika*, **33**, 305–325.
33. Cochran,W.G. and Cox,G.M. (1957) *Experimental Designs*. 2nd edn. Wiley.
34. Rieder,C.L. and Palazzo,R.E. (1992) Colcemid and the mitotic cycle. *J. Cell Sci.*, **102**, 387–392.
35. Skoufias,D.A., DeBonis,S., Saoudi,Y., Lebeau,L., Crevel,I., Cross,R., Wade,R.H., Hackney,D. and Kozielski,F. (2006) S-trityl-L-cysteine is a reversible, tight binding inhibitor of the human kinesin Eg5 that specifically blocks mitotic progression. *J. Biol. Chem.*, **281**, 17559–17569.
36. Zieve,G.W., Turnbull,D., Mullins,J.M. and McIntosh,J.R. (1980) Production of large numbers of mitotic mammalian cells by use of the reversible microtubule inhibitor Nocodazole. *Exp. Cell Res.*, **126**, 397–405.
37. Chou,C.F. and Omary,M.B. (1994) Mitotic arrest with anti-microtubule agents or okadaic acid is associated with increased glycoprotein terminal GlcNAc's. *J. Cell Sci.*, **107**, 1833–1843.
38. Bialojan,C. and Takai,A. (1988) Inhibitory effect of a marine-sponge toxin, okadaic acid, on protein phosphatases. Specificity and kinetics. *Biochem J.*, **256**, 283–290.
39. Anderson,M.J. and Whitcomb,P.J. (2007) *DOE Simplified: Practical Tools for Effective Experimentation*. 2nf edn. Productivity Press.
40. Pachnis,V., Pevny,L., Rothstein,R. and Costantini,F. (1990) Transfer of a yeast artificial chromosome carrying human DNA from Saccharomyces cerevisiae into mammalian cells. *Proc. Natl. Acad. Sci. U.S.A.*, **87**, 5109–5113.
41. Simpson,K. and Huxley,C. (1996) A shuttle system for transfer of YACs between yeast and mammalian cells. *Nucleic Acids Res.*, **24**, 4693–4699.
42. Eliceiri,B., Labella,T., Hagino,Y., Srivastava,A., Schlessinger,D., Pilia,G., Palmieri,G. and D'Urso,M. (1991) Stable integration and expression in mouse cells of yeast artificial chromosomes harboring human genes. *Proc. Natl. Acad. Sci. U.S.A.*, **88**, 2179–2183.
43. Pavan,W.J., Hieter,P. and Reeves,R.H. (1990) *Mol. Cell. Biol.*, **10**, 4163–4169.
44. Zhang,X.F., Wu,G.X., Chen,J.Q., Zhang,A.M., Liu,S.G., Jiao,B.H. and Cheng,G.X. (2005) Transfer of an expression YAC into goat fetal fibroblasts by cell fusion for mammary gland bioreactor. *Biochem. Biophys. Res. Commun.*, **333**, 58–63.
45. Rieder,C.L. and Cole,R. (2000) Microtubule disassembly delays the G2-M transition in vertebrates. *Curr. Biol.*, **10**, 1067–1070.
46. Noskov,V.N., Karas,B.J., Young,L., Chuang,R.Y., Gibson,D.G., Lin,Y.C., Stam,J., Yonemoto,I.T., Suzuki,Y., Andrews-Pfannkoch,C. *et al.* (2012) Assembly of large, high G+C bacterial DNA fragments in yeast. *ACS Synth. Biol.*, **1**, 267–273.
47. Lartigue,C., Vashee,S., Algire,M.A., Chuang,R.Y., Benders,G.A., Ma,L., Noskov,V.N., Denisova,E.A., Gibson,D.G., Assad-Garcia,N. *et al.* (2009) Creating bacterial strains from genomes that have been cloned and engineered in yeast. *Science*, **325**, 1693–1696.
48. Messerle,M., Crnkovic,I., Hammerschmidt,W., Ziegler,H. and Koszinowski,U.H. (1997) Cloning and mutagenesis of a herpesvirus genome as an infectious bacterial artificial chromosome. *Proc. Natl. Acad. Sci. U.S.A.*, **94**, 14759–14763.
49. Sheldrick,P., Laithier,M., Lando,D. and Ryhiner,M.L. (1973) Infectious DNA from herpes simplex virus: infectivity of double-stranded and single-stranded molecules. *Proc. Natl. Acad. Sci. U.S.A.*, **70**, 3621–3625.
50. Desai,P., DeLuca,N.A., Glorioso,J.C. and Person,S. (1993) Mutations in herpes simplex virus type 1 genes encoding VP5 and VP23 abrogate capsid formation and cleavage of replicated DNA. *J. Virol.*, **67**, 1357–1364.
51. Barber,G.N. (2011) Innate immune DNA sensing pathways: STING, AIMII and the regulation of interferon production and inflammatory responses. *Curr. Opin. Immunol.*, **23**, 10–20.
52. Ishikawa,H. and Barber,G.N. (2008) STING is an endoplasmic reticulum adaptor that facilitates innate immune signalling. *Nature*, **455**, 674–678.
53. Zhang,Y., Yeruva,L., Marinov,A., Prantner,D., Wyrick,P.B., Lupashin,V. and Nagarajan,U.M. (2014) The DNA sensor, cyclic GMP-AMP synthase, is essential for induction of IFN-beta during Chlamydia trachomatis infection. *J. Immunol.*, **193**, 2394–2404.
54. Karlin,S., Mocarski,E.S. and Schachtel,G.A. (1994) Molecular evolution of herpesviruses: genomic and protein sequence comparisons. *J. Virol.*, **68**, 1886–1902.
55. Kazuki,Y. and Oshimura,M. (2011) Human artificial chromosomes for gene delivery and the development of animal models. *Mol. Ther.*, **19**, 1591–1601.
56. Suzuki,T., Kazuki,Y., Oshimura,M. and Hara,T. (2016) Highly efficient transfer of chromosomes to a broad range of target cells using Chinese hamster ovary cells expressing murine leukemia virus-derived envelope proteins. *PLoS One*, **11**, e0157187.
57. Liskovykh,M., Lee,N.C., Larionov,V. and Kouprina,N. (2016) Moving toward a higher efficiency of microcell-mediated chromosome transfer. *Mol. Ther. Methods Clin. Dev.*, **3**, 16043.